Satellite coherent Doppler wind lidar performance simulation based on CALIOP measurements

Dong Wu, Pei Zhang, Suzhen Yu
College of Information Science and Engineering, Ocean University of China,
238 Songling Road, Qingdao, 266100, China

Abstract: A computer simulation tool using MATLAB has been developed based on the coherent Doppler lidar theory. The measurement performance of a satellite coherent Doppler wind lidar is computer simulated using the CALIOP measurements instead of aerosol model. Frehlich's two-parameter model is used to characterize the performance of the velocity estimates. The accuracy of radial wind velocity good estimates and the fraction of good estimates, depending on backscattered signals from aerosols, generally decrease with altitude. The simulation results demonstrated that a global wind profiling of the lower troposphere from space is feasible using a coherent Doppler wind lidar with achievable system design, appropriate performance setting and parameter selection.

Keywords: CALIOP, coherent Doppler wind lidar, performance simulation

1. Introduction

Global measurements of wind profiles are urgently needed for many meteorological studies. A spaceborne Doppler lidar is considered to be the observation system capable of such measurements in the troposphere. As early as the 1980's, a space-based coherent Doppler lidar system (Windsat) was proposed[1,2]. In the US, a hybrid lidar concept was selected for future spaceborne wind lidar system. Both a coherent lidar using heterodyne detection and an incoherent lidar using direct detection will be used for simultaneous wind measurements. The coherent Doppler lidar measures particulate scattering signals from aerosols which is suitable for lower altitude wind measurements.

The performance simulation of a spaceborne coherent Doppler lidar is important and requires correct modeling of the realistic characterization of aerosols and clouds. In most of the performance simulations of spaceborne Doppler lidar, the assumptions of ideal atmospheres are usually used. The performance of coherent Doppler lidar measurements has been simulated and evaluated for a modeled atmosphere with invariant aerosol backscatter [3,4] or varying aerosol backscatter [5,6]. The Doppler Lidar Simulation Model (DLSM) can simulate both coherent and incoherent Doppler wind lidar using modeled aerosol backscatter profiles [7,8]. A global aerosol backscatter distribution from CALIPSO lidar Level 2 aerosol profile data was used to simulate and assess the performance of wind speed measurements of a coherent Doppler wind lidar (CDWL) instead of the aerosol model [9].

The Cloud-Aerosol Lidar with Orthogonal Polarization (CALIOP) onboard the Cloud-Aerosol Lidar and Infrared Pathfinder Satellite Observation (CALIPSO) satellite has continuous worked for more than ten years. It has been providing a large amount of global cloud and aerosol measurement data with high vertical resolution [10,11]. In this study, the CALIOP Level 1064 nm attenuated backscatter profiles are used to simulate and assess the performance of wind speed measurements of a coherent Doppler wind lidar in cloud-free conditions based on the coherent detection theories.

2. Methodology

We follow mainly the coherent Doppler lidar theory summarized in [12]. The performance of the lidar velocity estimates is characterized by two parameters, the fraction of the bad estimates b and the RMS error of the good estimates g, as a function of coherent photoelectrons Φ_1:

$$b(\Phi_1) = \exp\left[-\left(\frac{\Phi_1}{b_0}\right)^{\alpha}\right], \tag{1}$$

$$g(\Phi_1) = w_{\upsilon,eff}\left\{\chi\left[1+\left(\frac{\Phi_1}{g_0}\right)^{\gamma}\right]^{-\delta} + \mu\right\}. \tag{2}$$

The coefficients in the above equations generally vary depending on the variations of the wind field, laser frequency stability, and transmitter and receiver geometries. Here, $\alpha = 1.364$, $b_0 = 11.42$, $\chi = 1.325$, $g_0 = 9747$, $\gamma = 0.9667$, $\delta = 209.2$, and $\mu = 0.04397$. $w_{\upsilon,\text{eff}}$ is the total effective spectral width in velocity space, and is related to the effective spectral width w_{eff} by $w_{\upsilon,\text{eff}} = \lambda\, w_{\text{eff}}/2$. λ is the laser wavelength. $w_{\upsilon,\text{eff}}$ is given by

$$w_{v,eff}^2 = s_{vr}^2 + s_{shr}^2 + w_v^2 + \sigma_{vLO}^2 \quad . \tag{3}$$

Following [12], $w_{\upsilon,\text{eff}}$=1.281 m/s, including the contributions from turbulence $s^2_{\text{vr}} = 0.5759$ (m/s)^2, wind shear $s^2_{\text{shr}} = 0.6592$ (m/s)^2, local laser frequency fluctuation $\sigma_{\text{vLO}} = 0.5$ m/s, and pulsed laser spectral widening $w_v = 0.3935$ m/s.

The number of received coherent photoelectrons Φ_1 can be estimated using

$$\Phi_1(R) = \frac{\eta_Q \beta(R) T^2(R) c E A_r \eta_H t_g}{2h\nu R^2}, \tag{4}$$

Where, R is the range probed by the leading edge of the pulse at time t, η_Q is the quantum efficiency, $\beta(R)$ is the backscatter coefficient, $T^2(R)$ the two-way atmospheric transmittance between the lidar and the atmosphere at R, c the speed of light, E the energy in each laser pulse, A_r the effective area of the receiving telescope, t_g the time interval of each range gate, and $t_g = Mt_s$, where t_s is the sampling interval and M is the number of complex lidar data samples in each range gate. $h = 6.626\times10^{-34}$ (J) is Planck constant, ν is the frequency of the laser. η_H is the heterodyne efficiency, defined as $\eta_H = C(R)/D(R)$, where $C(R)$ and $D(R)$ are the dimensionless coherent and incoherent responsivity, respectively. Both C(R) and D(R) can be expressed as a series that includes two physical representations of low-spatial-frequency (lf) behavior and high-spatial-frequency (hf) behavior [13], and the first order terms are given by

$$C_0(R) = C_{0,\text{lf}}(R) + \frac{1}{1+\left[\frac{k\rho_0^2(R)}{R}\right]^2} C_{0,\text{hf}}(R), \tag{5}$$

$$D_0(R) = D_{0,\text{lf}}(R) + \frac{1}{1+\left[\frac{k\rho_0^2(R)}{R}\right]^2} D_{0,\text{hf}}(R), \tag{6}$$

where

$$\rho_0(R) = \frac{1}{\left[Hk^2\int_0^R C_n^2\left(1-z/R\right)^{5/3}dz\right]^{3/5}} \tag{7}$$

is the transverse-field coherence length, $k = 2\pi/\lambda$ (rad m^{-1}), $H = 2.914383$, and C_n^2 is the refractive index structure constant. The impact of the atmospheric refractive turbulence on the heterodyne efficiency is small for the space-based measurements[9].

To calculate the number of received coherent photoelectrons Φ_1, in [9], the CALIOP Level 2 nighttime aerosol profile product, i.e., aerosol backscatter coefficients at 532 nm β_{532} with resolution of 60 m vertically and 5 km horizontally are used in the simulation. Then, the backscatter coefficients at 2.1 μm are derived from backscatter coefficients at 532 nm using a wavelength conversion function presented by Srivastava et al [14]. Different with that, here, we will focus our simulation on a 1064 nm CDWL measurement. The level 1 attenuated backscatter at 1064 nm can be directly used for the calculation of Φ_1 by using

$$\beta'_{1064nm}(R) = \beta_{1064nm}(R)T^2(R). \quad (8)$$

3. Simulation and results

The CALIOP level 1 data gives a set of calibrated attenuated backscatter profiles at 1064 nm with a vertical resolution of 60 m from -0.5 km to 20.2 km and 180 m between 20.2 km and 30.1 km[11]. The latest CALIOP Version 4.00 level 1 products are released in November 2014. The comparison shows that, the relative deviations of the attenuated backscatters between CALIOP level 1 Version 4.00 and Version 3.01 products for clouds and aerosols tend to positive values, and the changes are more obvious at nighttime than those at daytime for both clouds and aerosols. The mean relative deviation of 1064 nm attenuated backscatters for aerosol is 6.94% at daytime, and 10.92% at nighttime[16]. In this study, two months（Jul. and Nov. 2011） of CALIOP Version 4.00 L1B nighttime products are used for the calculation of the number of received coherent photoelectrons Φ_1 and the corresponding level 2 vertical feature mask (VFM) products are used for cloud-free data selection.

For data selection, the cloud-free range bins are defined as the bins that have the Feature Type of "clear air" and "aerosol" , but the cloud-free bins underneath a cloud bin are not included because the presence of clouds can attenuate the laser beam and consequently reduce the lidar signals backscattered from the air below the clouds. And, only the attenuated backscatters at 1064 nm less than 0.03 and greater than -0.02 are selected for the simulation. Latitude and longitude zonal-vertical distributions of mean cloud-free attenuated backscatters at 1064 nm are shown in Fig. 1.

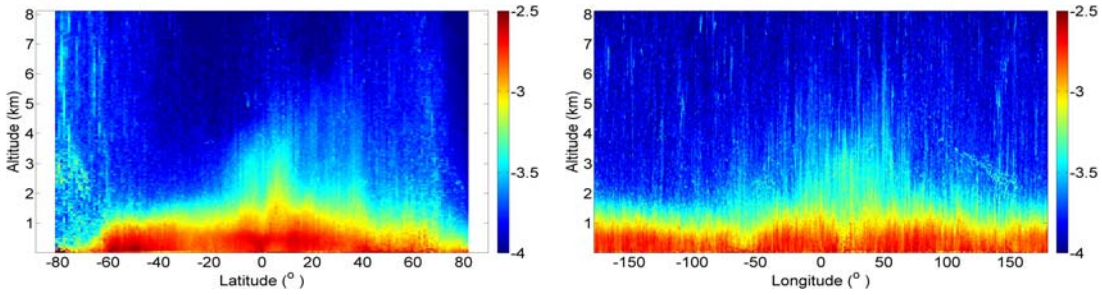

Fig. 1. Zonal-vertical distributions of mean attenuated backscatters at 1064 nm (log scale in km^{-1} sr^{-1})

A computer simulation tool using MATLAB has been developed based on the heterodyne detection theories mentioned above. The parameters of the spaceborne monostatic CDWL system are summarized in Table 1.

Table 1. System parameters of a space-based monostatic CDWL

Platform height = 410 km	Viewing angle = 45°
Laser wavelength λ = 1064 nm	Laser pulse energy E = 250 mJ
Radius of Gaussian-distributed laser beam and local oscillator $\sigma_L = \sigma_{LO} = 35$ cm	Radius of receiver lens $\sigma_R = 50$ cm
Focal length of the transceiver F = 578 km	Detector quantum efficiency $\eta_Q = 0.8$
Gate interval $t_g = 7.5$ μs	Sampling interval $t_s = 0.05$ μs
Range-gate length $R_g = 1.125$km	Vertical resolution $Z_g = 0.795$ km
Effective spectral width, $w_{v,eff} = 1.281$ m s^{-1}	Normalized spectral width Ω = 18.05

Based on the vertical distributions of mean attenuated backscatters at 1064 nm from CALIOP level 1 data shown in Fig. 1, the spaceborne CDWL given in Table 1 is simulated. The main parameters and conditions follow [9] and [12]. The refractive index structure constant C_n^2 measured in clear-air conditions in winter at nighttime [17] is used for the η_H calculation. Fig. 2 gives simulated latitude and longitude zonal-vertical distributions of received number of coherent photoelectrons Φ_1. It shows a strong similarity with Fig. 1 because a CDWL uses aerosol as a tracer of wind. The received coherent photoelectron number can reach several thousands in the boundary layer less than1 km where most of the

atmospheric aerosol is distributed, and decreases with altitude because the aerosol loading decreases with altitude. In most area shown in Fig.2, the received coherent photoelectron number is larger than 100.

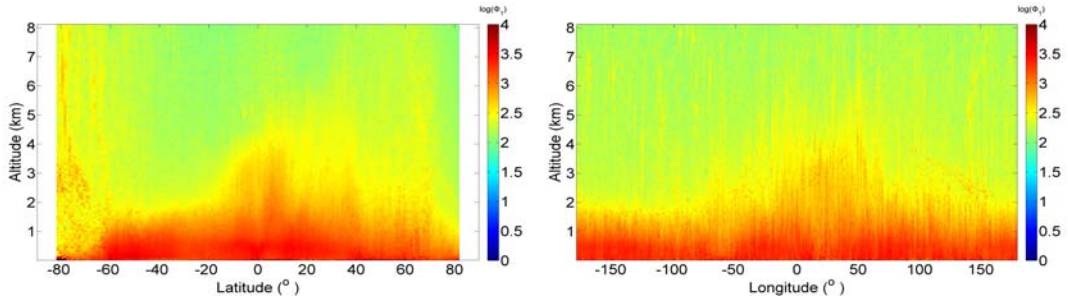

Fig. 2. Simulated zonal-vertical distributions of received number of coherent photoelectrons Φ_1

The latitude and longitude zonal-vertical distributions of the calculated fraction of bad estimates b and radial velocity RMS error of good velocity estimates g are presented in Fig. 3 and Fig. 4, respectively. Fig. 3 shows that b is less than 0.1 in most of the atmospheric aerosol is distributed. The altitudes of b = 0.1 where a wind measurement with a faction of 10% bad estimates decreases as approaching the two poles where the aerosol loading is small. It is seen that the accuracy of radial wind velocity good estimates g increases as Φ_1 decreases (Fig. 4 vs. Fig. 1), and can reach an altitude of 2 km with radial velocity RMS error less than 0.3 m/s except in the areas of the two poles.

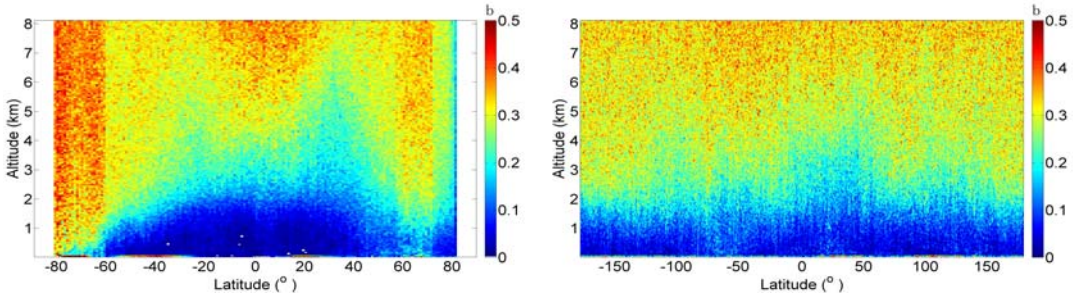

Fig. 3. Zonal-vertical distributions of the calculated fraction of bad estimates *b*

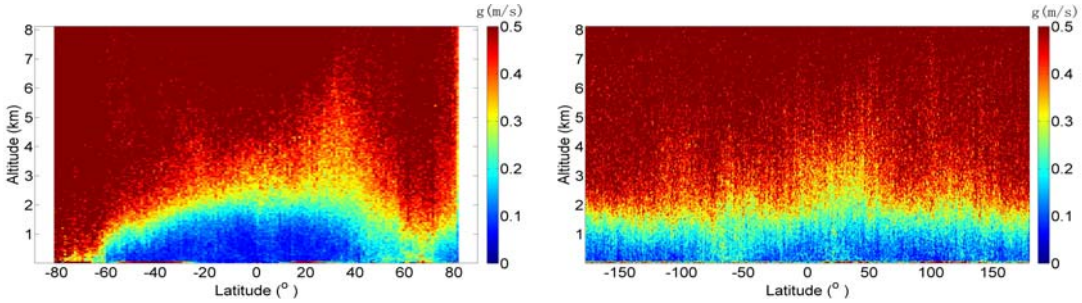

Fig. 4. Zonal-vertical distributions of RMS error of good velocity estimates g in m/s

4. Conclusions

The single-shot measurements of a 1064 nm CDWL in cloud- free conditions are simulated using latitude and longitude zonal-vertical distributions of mean attenuated backscatters at 1064 nm from two months （Jul. and Nov. 2011）of CALIOP Version 4.00 level 1 nighttime profile products. The corresponding feature types from CALIOP level 2 vertical feature mask (VFM) products are used for cloud-free data selection.

The simulation results show that the distributions of calculated fraction of bad estimates b and radial velocity RMS error of good velocity estimates g show strong similar patterns with the distribution of attenuated backscatters at 1064 nm because a CDWL uses aerosol as a tracer of wind. The altitude of accuracy of radial wind velocity good estimates g less than 0.3 m/s can reach an altitude of 2 km except in the areas of the two poles.

5. Acknowledgements

This work is supported by the National Natural Science Foundations of China (Grant No.41376180). The authors acknowledge the Atmospheric Science Data Center (ASDC) at the NASA Langley Research Center for providing the CALIPSO data used in this paper.

6. References

[1] Huffaker RM, Lawrence TR, Post MJ, Priestley JT, Hall FF, Richter RA, et al, "Feasibility studies for a global wind measuring satellite system (Windsat): Analysis of simulated performance," Appl Opt 23, 2523-2536 (1984).

[2] Menzies RT, "Doppler lidar atmospheric wind sensors: A comparative performance evaluation for global measurement applications from earth orbit," Appl Opt 25, 2546-2553 (1986).

[3] Frehlich RG, Yadlowsky MJ, "Performance of mean frequency estimators for Doppler radar and lidar," J Atmos Oceanic Technol, 11, 1217-1230 (1994).

[4] Lottman BT, Frehlich RG, "Evaluation of coherent Doppler lidar velocity estimators in non-stationary regimes," Appl Opt36, 7906-7918 (1997).

[5] Frehlich RG, "Simulation of coherent Doppler lidar performance for space-based platforms," J Appl Meteor 39(2), 245-262 (2000).

[6] Frehlich RG, "Errors for space-based Doppler lidar wind measurements: Definition, performance, and verification," J Atmos Oceanic Technol18,1749-1772 (2001).

[7] Wood S, Emmitt GD,Greco S, "DLSM: A coherent and direct detection lidar simulation model for simulating space-based and aircraft-based lidar winds," In:Gary W. Kamerman, Upendra N. Singh, Christian Werner,Vasyl V, Molebny, Editors. Laser Radar Technology and Applications V. Proceedings of SPIE 4035, 2-12 (2000).

[8] The Community Doppler Lidar Simulation Model (DLSM). Available from:

http://www.swa.com/10-services/environment-laser-division/365-dlsm-version-4-4

[9] Wu D, Tang J, Liu Z, Hu Y, "Simulation of coherent Doppler wind lidar measurement from space based on CALIPSO lidar global aerosol observations," J Quant Spectrosc Radiat Transfer122, 79-86 (2013).

[10] Winker DM, Hunt WH, McGill MJ, "Initial performance assessment of CALIOP," Geophys Res Lett 34, 228-262 (2007).

[11] Winker DM, Pelon J, Coakley Jr JA, Ackerman SA, Charlson RJ, Colarco PR, et al, "The CALIPSO mission: a global 3D view of aerosols and clouds," Bull Am Meteorol Soc 91, 1211-1229 (2010).

[12] Frehlich R, "Velocity error for coherent Doppler lidar with pulse accumulation," J Atmos Oceanic Technol 21, 905-920 (2004).

[13] Frehlich RG, Kavaya MJ, "Coherent laser radar performance for general atmospheric refractive turbulence," Appl Opt 30(36), 5325–5352 (1991).

[14] Srivastava V, Rothermel J, Clarke AD, Spinhirne JD, Menzies RT, Cutten DR, et al, "Wavelength dependence of backscatter by use of aerosol microphysics and lidar data sets: application to 2.1-μm wavelength for space-based and airborne lidars," Appl Opt 40(27), 4759–4769 (2001).

[15] Kacenelenbogen M, Vaughan M A, Redemann J, et al, " An accuracy assessment of the CALIOP/CALIPSO version 2/version 3 daytime aerosol extinction product based on a detailed multi-sensor, multi-platform case study," Atmos Chem Phys 11(11), 3981-4000 (2011).

[16] Zhang T, Wu D, "Differences between attenuated backscatters obtained from CALIOP version 3 and latest version 4 products for clouds and aerosols", Laser & Optoelectronics Progress, 53, 060102 (2016).

[17] Fairall CW, Frish AS. "Diurnal and annual variation in mean profiles of C_n^2," NOAA Technical Memorandum ERL WPL-195. National Oceanic and Atmospheric Administration, Boulder, Co. (1991).